Journal of Biomechanics 110 (2020) 109915

Contents lists available at ScienceDirect

Journal of Biomechanics

journal homepage: www.elsevier.com/locate/jbiomech
www.JBiomech.com

Tibio-femoral kinematics of the healthy knee joint throughout complete cycles of gait activities

Barbara Postolka [a,1], Pascal Schütz [a,1], Sandro F. Fucentese [b], Michael A.R. Freeman [c,†], Vera Pinskerova [d], Renate List [a,e], William R. Taylor [a,*]

[a] Institute for Biomechanics, ETH Zürich, Zürich, Switzerland
[b] Balgrist University Hospital, Zürich, Switzerland
[c] Royal London Hospital, London, United Kingdom
[d] Medical Faculty, Charles University, Prague, Czech Republic
[e] Human Performance Lab, Schulthess Clinic, Zürich, Switzerland

ARTICLE INFO

Article history:
Accepted 25 June 2020

Keywords:
In vivo knee kinematics
Tibio-femoral kinematics
Fluoroscopy
Gait
Stair descent
Ramp descent

ABSTRACT

Accurate assessment of 3D tibio-femoral kinematics is essential for understanding knee joint functionality, but also provides a basis for assessing joint pathologies and the efficacy of musculoskeletal interventions. Until now, however, the assessment of functional kinematics in healthy knees has been mostly restricted to the loaded stance phase of gait, and level walking only, but the most critical conditions for the surrounding soft tissues are known to occur during high-flexion activities. This study aimed to determine the ranges of tibio-femoral rotation and condylar translation as well as provide evidence on the location of the centre of rotation during multiple complete cycles of different gait activities.

Based on radiographic images captured using moving fluoroscopy in ten healthy subjects during multiple cycles of level walking, downhill walking and stair descent, 3D femoral and tibial poses were reconstructed to provide a comprehensive description of tibio-femoral kinematics.

Despite a significant increase in joint flexion, the condylar antero-posterior range of motion remained comparable across all activities, with mean translations of 6.3–8.3 mm and 7.3–9.3 mm for the medial and lateral condyles respectively. Only the swing phase of level walking and stair descent exhibited a significantly greater range of motion for the lateral over the medial compartment. Although intra-subject variability was low, considerable differences in joint kinematics were observed between subjects. The observed subject-specific movement patterns indicate that accurate assessment of individual pre-operative kinematics together with individual implant selection and/or surgical implantation decisions might be necessary before further improvement to joint replacement outcome can be achieved.

1. Introduction

Kinematics of the human knee are guided by an interconnected system of bones, soft tissue structures and muscles acting around the joint. The resulting joint function in healthy knees is known to exhibit motion in all six degrees of freedom, presenting a complex set of translations and rotations (Andriacchi et al., 1998). Accurate knowledge of tibio-femoral movement can hence provide critical information for assessing knee joint functionality (Akbarshahi et al., 2010), but also lay the foundations for understanding joint pathologies and musculoskeletal interventions. Total knee arthroplasty (TKA) or ligament reconstruction surgeries generally aim to restore pain-free functionality to the joint, based on physiological kinematics. However, the motion patterns of the native tibio-femoral joint itself are still discussed controversially (Dennis et al., 2001; Gray et al., 2019; Komistek et al., 2003; Koo and Andriacchi, 2008; Kozanek et al., 2009). Nevertheless, novel implant designs have been introduced that aim to mimic healthy joint kinematics, even though a comprehensive understanding of tibio-femoral kinematics during different gait activities remains missing.

While early studies used cadaveric material to examine tibio-femoral motion, optical motion capture using skin-mounted markers has become commonplace for assessing dynamic joint function. However, these measurements are known to be critically affected

* Corresponding author at: ETH Zürich, Institute for Biomechanics, Leopold-Ruzicka-Weg 4, 8093 Zürich, Switzerland.
E-mail address: bt@ethz.ch (W.R. Taylor).
[1] BP and PS contributed equally to this manuscript.
† Died 14th Sept 2017.

https://doi.org/10.1016/j.jbiomech.2020.109915
0021-9290/© 2020 The Authors. Published by Elsevier Ltd.

by soft tissue artefact (STA) (Andriacchi et al., 1998; Cappozzo et al., 2005; Taylor et al., 2005). Errors associated with STA can be avoided using pins screwed directly into the subjects' bones (Lafortune et al., 1992; Reinschmidt et al., 1997), but such procedures are highly invasive and therefore limited to small cohort studies. To directly assess tibio-femoral kinematics in a less invasive manner, single-plane (Dennis et al., 2001; Galvin et al., 2019; Grieco et al., 2016; List et al., 2017; Moewis et al., 2016; Moro-oka et al., 2008) and dual-plane (Anderst et al., 2009; Guan et al., 2016; Kozanek et al., 2009; Li et al., 2008) fluoroscopic analyses have provided valuable and accurate data. The predominant drawback of most systems, however, relates to the small size and static nature of the intensifier, hence restricting measurements to a limited field-of-view. Consequently, most studies have analysed quasi-static activities such as knee bending, squatting and sit-to-stand or assessed only a portion of the gait cycle (Dennis et al., 2001; Galvin et al., 2019; Grieco et al., 2018; Komistek et al., 2003; Kono et al., 2018; Kozanek et al., 2009; Moro-oka et al., 2008; Yamaguchi et al., 2009). To overcome the limitations of static imaging set-ups, procedures to enhance the fluoroscopic field-of-view have been investigated (Li et al., 2008). Moreover, mobile fluoroscopic systems have emerged that allow tracking of the knee during dynamic movements (Yamokoski and Banks, 2011) and consecutive cycles of gait activities (Guan et al., 2016; List et al., 2017).

Due to their strong radiographic image contrast and associated ease of 2D/3D registration to fluoroscopic images, the kinematics of total knee replacements have been studied in detail (Banks and Hodge, 1996; Dennis et al., 2001; Grieco et al., 2018; Guan et al., 2017; Schütz et al., 2019a, 2019b). The movement patterns of the natural knee have, however, proven far more difficult to access. While most available studies have evaluated the loaded stance phase of walking (Benoit et al., 2007; Dennis et al., 2001; Komistek et al., 2003; Koo and Andriacchi, 2008; Kozanek et al., 2009; Reinschmidt et al., 1997), only few studies have successfully examined tibio-femoral kinematics over a complete cycle of walking (Andriacchi et al., 1998; Gray et al., 2019; Lafortune et al., 1992; Li et al., 2008). While consistent findings were presented for joint flexion, with a first peak observed at contralateral toe-off and a maximum knee flexion shortly after toe-off (Andriacchi et al., 1998; Benoit et al., 2007; Farrokhi et al., 2012; Gray et al., 2019; Kozanek et al., 2009; Lafortune et al., 1992; Li et al., 2009; Li et al., 2008; Reinschmidt et al., 1997), contradictory patterns were reported for the other two rotations. Most studies observed an internally rotated tibia at heel-strike, followed by further internal rotation during early stance phase, reaching a first peak shortly after contralateral toe-off (Andriacchi et al., 1998; Farrokhi et al., 2012; Gray et al., 2019; Kozanek et al., 2009; Lafortune et al., 1992; Li et al., 2008; Reinschmidt et al., 1997). The tibia is then thought to rotate externally through mid-stance, before rotating internally once again prior to toe-off (Gray et al., 2019; Kozanek et al., 2009; Lafortune et al., 1992; Li et al., 2008; Reinschmidt et al., 1997). Contrary to this common understanding of knee motion, tibial external rotation during early stance phase was described in two studies (Benoit et al., 2007; Komistek et al., 2003), where tibial internal rotation during mid-stance was followed by external rotation from 66% of the stance phase until toe-off. In the few studies that were able to assess the unloaded swing phase, peak tibial internal rotation was found shortly after toe-off, followed by external rotation until just before heel-strike, with tibial internal rotation occurring in preparation for the following heel-strike (Andriacchi et al., 1998; Gray et al., 2019; Lafortune et al., 1992). Throughout the complete gait cycle, minimal changes in abduction/adduction were observed, but with clear subject-specific differences (Andriacchi et al., 1998; Kozanek et al., 2009; Lafortune et al., 1992).

Only few studies have examined the antero-posterior (A-P) translation of the two femoral condyles relative to the tibia individually. Here, a larger translation has generally been observed for the lateral compared to the medial condyle during the loaded stance phase (Dennis et al., 2001; Komistek et al., 2003), as well as over complete gait cycles (Gray et al., 2019), indicating an overall medial centre of rotation (CoR). In contrast, Koo and Andriacchi (2008) observed more translation of the medial compared to the lateral condyle during the loaded stance phase of gait, which was later supported by Kozanek and co-workers (2009).

Beyond these reports, quantifying knee motion during more challenging activities of daily living such as downhill walking and stair descent are critical for understanding knee function. In the limited literature, no consistent trend of A-P translation of the medial versus the lateral condyle was reported for either of the two activities, and analysis of the unloaded swing phase remains missing (Dennis et al., 2001; Farrokhi et al., 2014; Komistek et al., 2003).

As a result, tibio-femoral movement patterns during functional gait activities are still discussed controversially. Importantly, comparison of condylar A-P translation is complicated by the method used for analysing the movement: the tibio-femoral contact path (Dennis et al., 2001; Gray et al., 2019; Komistek et al., 2003), geometric condylar centres (Gray et al., 2019; Kozanek et al., 2009), or points on the transepicondylar axis (Kozanek et al., 2009) have all been used to describe condylar translation, plausibly also contributing to the inconsistent observations. However, it also remains unclear whether the observed variations resulted from differences in performing the activities, the cohorts studied, or simply because of variability in soft tissue structure or anatomy. Therefore, the aim of this study was to determine the ranges of tibio-femoral rotation and condylar translation during complete cycles of free level walking, downhill walking and stair descent, as well as provide evidence on the location and possible movement of the centre of joint rotation in the transverse plane in healthy knees.

2. Methods

2.1. Subjects

Ten subjects (5 female/5 male, aged 23.7 ± 3.2 years, BMI 21.7 ± 2.2 kg/m^2) provided written, informed consent to participate in this study, which was approved by the local ethics committee (KEK-ZH-Nr. 2016-00410). All subjects underwent a clinical knee examination (including testing of ligament condition) by an experienced knee surgeon, and subject-specific limb alignment (mean varus angle of 0.6 ± 1.4°) was evaluated using a biplanar X-ray system (EOS imaging, France) in a standing position (Folinais et al., 2013). Subjects with significant problems at the lower extremities or exhibiting a limb alignment >3° varus/valgus were excluded from this study.

2.2. Measurement Set-Up

Tibio-femoral kinematics were assessed using the ETH moving fluoroscope (List et al., 2017), synchronised with a 22 camera optical motion capture system (Vicon MX System, Oxfords Metrics Group, UK) as well as five floor-mounted force plates (Kistler AG, Switzerland), while an additional two mobile force plates instrumented the ramp and stairs respectively (Fig. 1). The subjects performed all motion tasks in a pair of self-selected sports shoes.

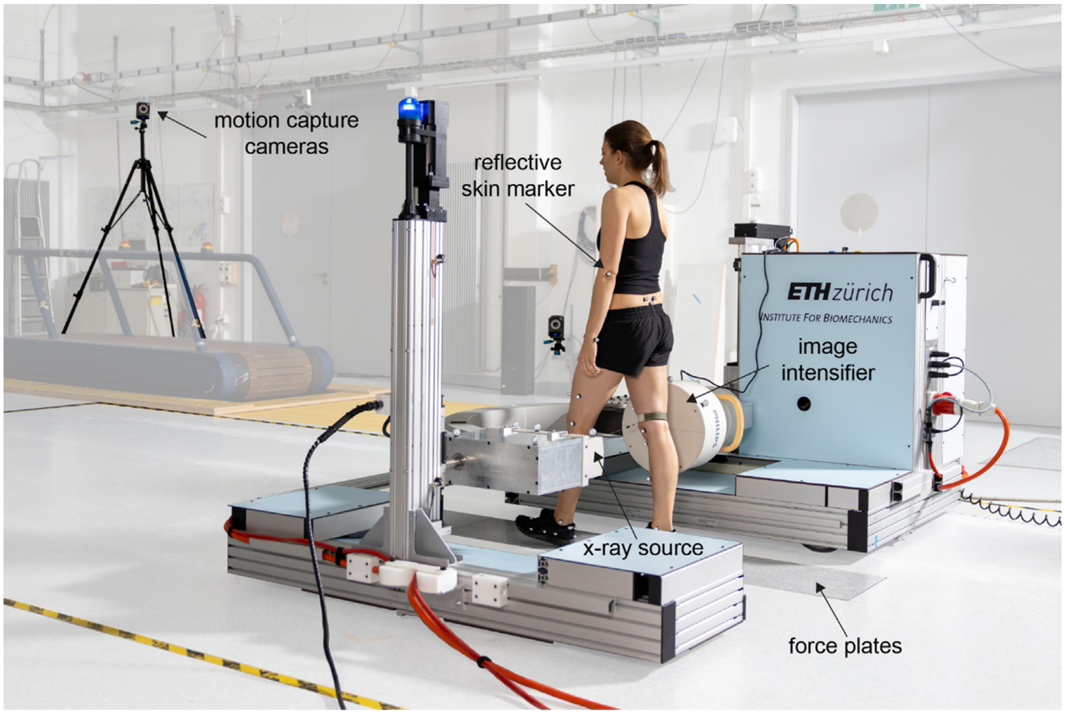

Fig. 1. Measurement set-up during level walking. Radiographic images of the knee were captured using a moving fluoroscope, imaging at 25 Hz (1 ms shutter time) with an image resolution of 1000 × 1000 pixels (List et al., 2017; Foresti, 2009). The moving fluoroscope was equipped with five optical markers on the x-ray source and six on the image intensifier to track its position (List et al., 2017). Fifty-five skin markers, placed at specific anatomical locations (List et al., 2013), were tracked at 100 Hz using a 22 camera system (Vicon MX system, Oxford Metrics Group, UK). Five force plates embedded in the floor (decoupled from surrounding ground) and two mobile force plates mounted on the ramp and stairs (Kistler Instrumentation, Switzerland) were used to measure undisturbed ground reaction forces at a sampling frequency of 2000 Hz.

2.3. Motion tasks

After a standing trial and activity-specific familiarisation trials, all subjects were measured throughout at least five valid cycles each of straight level walking, downhill walking (10° declined slope), and stair descent (three steps, each 18 cm in height) – in this study collectively considered to be gait activities. Trials were considered valid when the knee remained within the field-of- view of the image intensifier throughout the stance as well as the swing phase, and all force plates were hit correctly. The ground reaction forces were used to determine heel-strike and toe-off with a threshold of 25 N. For downhill walking, the second heel-strike, marking the end of swing phase, was defined based on the trajectory of a heel marker. Overall, for each participant the mean dose area product (DAP) was 7.9 ± 1.2 $Gycm^2$ (diameter image intensifier 30.5 cm) leading to a total average effective dose of 0.11 ± 0.02 mSv for the fluoroscopic measurement.

2.4. 3D tibio-femoral kinematics

Subject-specific volumetric models were obtained based on a CT scan of each subject's knee (~20 cm proximal/distal of the joint line, resolution 0.5 × 0.5 mm, slice thickness 1 mm), followed by manual segmentation of the data using the open-source software MITK-GEM (Pauchard et al., 2016). All fluoroscopic images were distortion corrected and the optical projection parameters (focal distance, principal point) were determined (Foresti, 2009). The 3D position and orientation of the femur and tibia were evaluated using a semi-automatic 2D/3D registration software (Postolka et al., 2020), with reported mean absolute errors of <1° for rotations around all three axes, <0.6 mm for in-plane, and <7.1 mm for out-of-plane translations using artificial bones with radiopaque image properties.

Local femoral and tibial anatomical coordinate systems were established to calculate relative tibio-femoral rotations (Fig. 2A and B) (Grood and Suntay, 1983). The functional flexion axis (FFA) was defined based on kinematics derived from the fluoroscopic imaging data of a maximal deep knee bending trial using the symmetrical axis of rotation approach (Ehrig et al., 2007). Condylar A-P location was calculated based on a medial (FFA_P_{med}) and lateral (FFA_P_{lat}) point on the functional flexion axis of the femur (Fig. 2C). Translation of each femoral condyle was then described as the movement of these points with respect to the mid-coronal plane of the tibia. All A-P translations were scaled using a subject-specific coefficient, scaled to a ratio of the mean condylar width divided by the subject's condylar width (Gray et al., 2019). To allow comparison and interpretation throughout complete gait cycles, tibio-femoral kinematic data was linearly interpolated to 101 data points. To allow comparison of joint kinematics against other studies, tibio-femoral translation is additionally presented using the nearest point (N_P) approach (same normalisation and interpolation) on the surface of each femoral condyle (N_P_{med} and N_P_{lat}) relative to a plane parallel to the tibial articular surface, as described by Asano and co-workers (2001).

Finally, the CoR in the transverse plane was calculated using the symmetrical centre of rotation estimation based on the locations of FFA_P_{med} and FFA_P_{lat} (Ehrig et al., 2006).

2.5. Statistics

A total of four mixed-model analysis of variances (ANOVAs) with subject as random effect were performed. Three mixed-model ANOVAs were performed to investigate the influence of the task and gait-phase on the ranges of tibio-femoral rotation using the ranges of rotation (flexion/extension, ab/adduction, tibial internal/external) as the dependent variables, with task (three

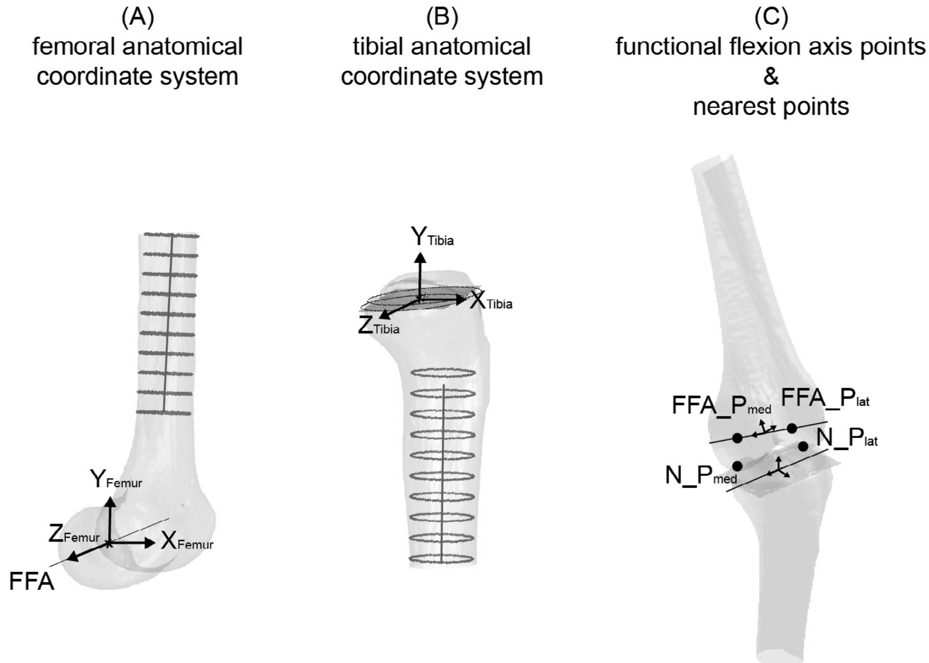

Fig. 2. (A) Femoral anatomical coordinate system pictured in a left femur. Based on the fluoroscopic imaging data of a maximal deep knee bending trial, the functional flexion axis (FFA) was defined using the functional symmetrical axis of rotation approach (Ehrig et al., 2007). The origin was defined as the midpoint between the most medial and lateral point of the femur on the FFA. The medio-lateral axis (Z_{Femur}), was oriented along the FFA, pointing medially. A cylinder (depicted as multiple circles) was then fitted to the most proximal 10 cm of the femoral shaft, defining the shaft axis. The antero-posterior axis (X_{Femur}) was orthogonal to Z_{Femur} and the shaft axis. In right knees, X_{Femur} pointed posterior, while in left knees it was directed anteriorly. The longitudinal axis (Y_{Femur}) was orthogonal to both X_{Femur} and Z_{Femur} to complete the right-handed coordinate system. (B) Tibial anatomical coordinate system pictured in a left tibia. A plane parallel to the posterior tibial slope was constructed, resecting the condylar cartilage. Two circles were manually fitted in the plane, such that the maximum possible circle perimeter fitted to the tibial cortex. The midpoint between the two circles' origins was set as the origin of the tibial anatomical coordinate system. Similar to the femur, a cylinder was fitted to the most distal 10 cm of the tibial shaft (depicted as multiple circles). However, for the tibia, the longitudinal axis (Y_{Tibia}) was consistent with the orientation of the shaft axis, but passed through the origin. The antero-posterior axis (X_{Tibia}) was orthogonal to Y_{Tibia} and the line connecting the circle centres. Similar to the femur, the X_{Tibia} pointed posteriorly in right knees, but anteriorly in left knees. The medio-lateral axis (Z_{Tibia}) was orthogonal to the X_{Tibia} and Y_{Tibia} to complete the right-handed coordinate system. (C) The nearest points (N_P_{med} & N_P_{lat}) between the femoral condyles and the tibial plane were calculated as the weighted means of the ten nearest points (mean point separation 0.4 mm) for the medial and the lateral condyles. Two points on the functional flexion axis (FFA_P_{med} & FFA_P_{lat}) were then defined based on the projection of N_P_{med} & N_P_{lat} during standing onto the FFA. These points were used to describe condylar antero-posterior (A-P) translation relative to the tibia.

levels: level walking, downhill walking, stair descent) and gait-phase (two levels: stance phase, swing phase) as independent variables. One ANOVA was applied to test the effect of task, side, and gait-phase on the range of A-P translation (FFA_P approach). Here, the range of A-P translation was set as the dependent variable, while task (three levels: level walking, downhill walking, stair descent), gait-phase (two levels: stance phase, swing phase) and side (two levels: medial A-P, lateral A-P) were set as the independent variables. The least significant differences approach was used for post-hoc comparisons and the levels of significance were corrected for multiple comparisons, starting at $\alpha = 0.05$, using Bonferroni correction. No statistical tests were performed for the A-P translation of the N_P approach. Statistics were conducted in SPSS (SPSS 24, IBM, USA).

3. Results

Mean average velocities over the complete gait cycle were 0.8 7 ± 0.06 m/s during level walking, 0.81 ± 0.07 m/s during downhill walking, and 0.58 ± 0.05 m/s for stair descent.

3.1. Tibio-femoral rotations

During standing, a mean knee flexion of −2.6 ± 5.6° and tibial external rotation of 2.8 ± 9.9° (range −13.1° internal to 16.4° external) were recorded.

As expected, a significant increase in range of joint flexion was observed from level walking to downhill walking and stair descent (Table 1A). For all three activities, the knee joint was slightly flexed at heel-strike, followed by an activity-specific flexion/extension behaviour, with peak knee flexion occurring shortly after toe-off (level walking: 62.8 ± 5.5°; downhill walking: 70.1 ± 4.7°; stair descent 95.0 ± 5.7°) (Fig. 3).

After heel-strike, the tibia generally rotated internally during the stance phase, reaching a maximum internal rotation shortly before toe-off (level walking: −9.9 ± 6.9°, downhill walking: −10.6 ± 7.7°, stair descent: −12.3 ± 7.6°) followed by an external rotation in preparation for the subsequent heel-strike (Fig. 3). Initial tibial internal/external rotation at heel-strike was highly subject-specific, with individual values ranging from −14.5° internal to 11.1° external rotation between the three activities. However, each subject exhibited consistent internal/external rotation characteristics, with a mean standard deviation (SD) of 1.5–3.4° across all subjects.

Repeatable ab/adduction was found for the individual subjects (mean subject SDs: 0.9–1.8°), but these were highly individual, and no clear ab/adduction patterns could be established over a complete gait cycle for any of the activities (Supplementary material: Fig. S1).

3.2. Condylar translation

During standing, the mean FFA_P_{med} (−10.6 ± 7.0 mm) and FFA_P_{lat} (−8.7 ± 5.7 mm) over all subjects were located posterior to the tibial mid-coronal plane.

Table 1
Range of motion for (A) all three tibio-femoral rotations. Flex/ex: flexion/extension, int/ext: tibial internal/external rotation, ab/add: abduction/adduction (B) Antero-posterior (A-P) translation for FFA_P_{med} and FFA_P_{lat} (C) A-P translation for N_P_{med} and N_P_{lat}. Mean and standard deviations across all 10 subjects are presented for the loaded stance and unloaded swing phases of level walking, downhill walking and stair descent.

	RoM [°]	Rotation during the loaded stance phase			Rotation during the unloaded swing phase		
		flex/ex	int/ext	ab/add	flex/ex	int/ext	ab/add
(A)	Level Walking	39.1 ± 4.8 [*a,b]	12.9 ± 2.1	5.4 ± 1.5 [*d]	65.6 ± 4.0 [*f,g]	12.2 ± 3.9	6.3 ± 1.7
	Downhill Walking	55.3 ± 3.2 [*a,c]	13.5 ± 3.1	5.2 ± 1.1 [*e]	72.0 ± 3.4 [*f,h]	11.6 ± 3.3 [*i]	6.2 ± 1.8
	Stair Descent	79.9 ± 5.2 [*b,c]	13.0 ± 2.6	6.5 ± 1.2 [*d,e]	93.1 ± 4.6 [*g,h]	13.3 ± 2.4 [*i]	5.6 ± 1.3

	RoM [mm]	A-P translation during the loaded stance phase		A-P translation during the unloaded swing phase	
		FFA_P_{med}	FFA_P_{lat}	FFA_P_{med}	FFA_P_{lat}
(B) FFA_P	Level Walking	8.3 ± 1.8 [**k]	8.2 ± 1.4	6.6 ± 1.6 [**k,o]	8.1 ± 1.8 [**o]
	Downhill Walking	8.0 ± 2.5 [**l]	8.5 ± 1.5 [**m]	6.3 ± 1.7 [**l]	7.3 ± 1.9 [**m,q]
	Stair Descent	8.2 ± 2.6 [**n]	9.3 ± 2.1	6.7 ± 1.7 [**n,p]	9.1 ± 2.2 [**p,q]

	RoM [mm]	A-P translation during the loaded stance phase		A-P translation during the unloaded swing phase	
		N_P_{med}	N_P_{lat}	N_P_{med}	N_P_{lat}
(C) N_P	Level Walking	10.3 ± 3.2	15.5 ± 6.1	13.3 ± 4.3	21.7 ± 8.5
	Downhill Walking	9.5 ± 2.5	17.4 ± 8.8	13.0 ± 4.2	21.8 ± 8.7
	Stair Descent	9.7 ± 2.1	15.4 ± 6.4	10.7 ± 3.3	20.9 ± 6.3

*Significant differences are presented between lettered pairs (a–i) based on the adjusted level of significance of α = 0.017.
**Significant differences are presented between lettered pairs (k–p) based on the adjusted level of significance of α = 0.0083.
No statistical tests were conducted for the N_P approach.

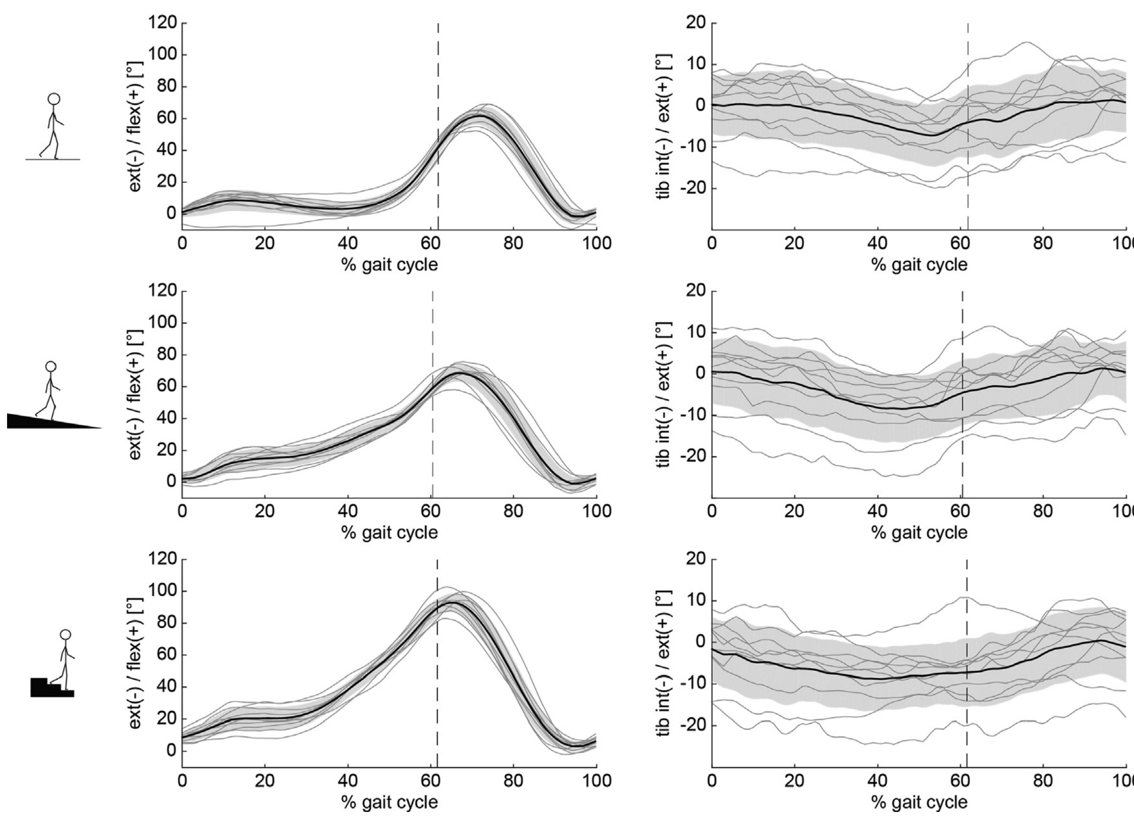

Fig. 3. Tibio-femoral flexion/extension (flex/ex) and tibial internal/external rotations (tib int/ext) throughout complete cycles of level walking (top), downhill walking (middle) and stair descent (bottom). The mean across all subjects (black line), standard deviations across all subjects (grey shading), as well as means for every subject (dark grey lines) are presented. The average instance of toe-off across all subjects is indicated as a vertical dashed line.

Following a short posterior translation after heel-strike, FFA_P_{med} moved anteriorly, peaking shortly before toe-off for both level and downhill walking. This motion was followed by a short posterior and again anterior translation, reaching a second peak before returning to its initial position at heel-strike (Fig. 4). For all three activities, a significant difference was found for the amount of A-P translation of the FFA_P_{med} between the stance and the swing phases (Table 1B). The FFA_P_{lat} moved posteriorly after heel-strike, reaching a minimum around toe-off. Extension of the knee during the unloaded swing phase was then associated with an anterior translation of the FFA_P_{lat} for all three activities and all subjects (Fig. 4). Overall, FFA_P_{med} and FFA_P_{lat} showed

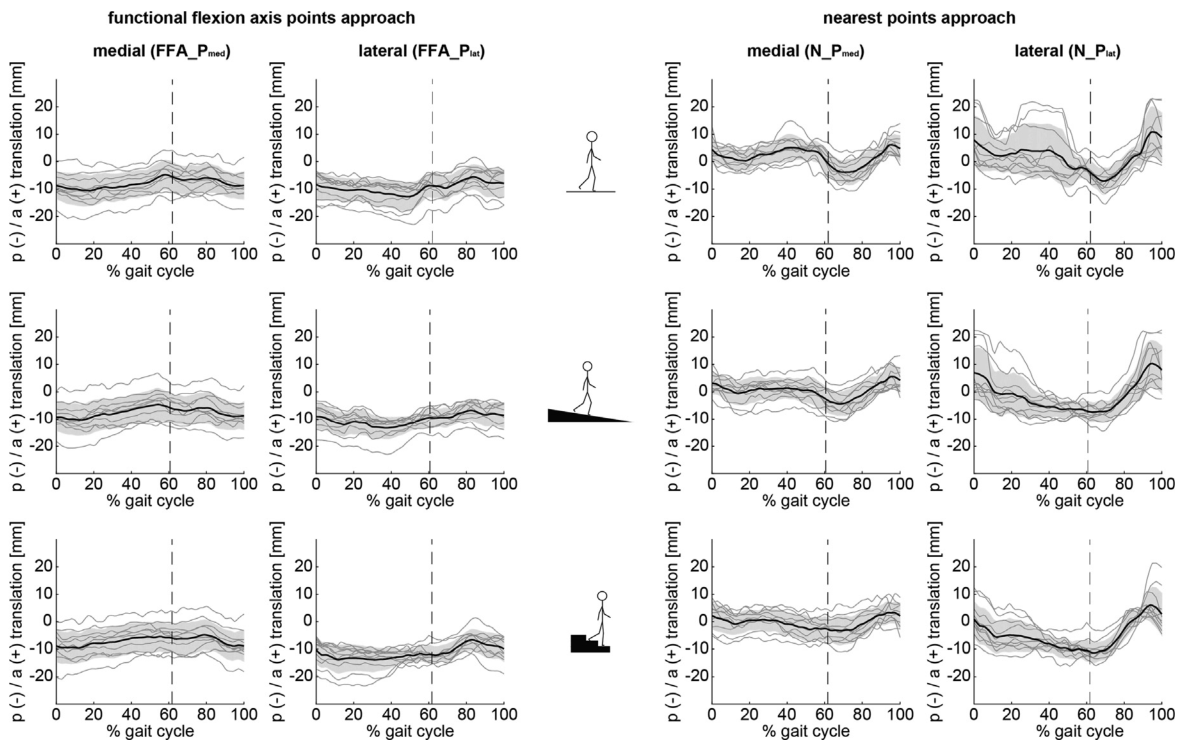

Fig. 4. Antero (a) – posterior (p) translation of the medial and lateral functional flexion axis points (left) as well as the nearest points (right) throughout complete cycles of level walking (top), downhill walking (middle) and stair descent (bottom). The mean across all subjects (black line), standard deviations across all subjects (grey shading), as well as means for every subject (dark grey lines) are presented. The average instance of toe-off across all subjects is indicated as a vertical dashed line.

comparable ranges of A-P translation, with only the swing phase of level walking and stair descent showing significant differences (Table 1B). Intra-subject repeatability was high for both FFA_P_{med} and FFA_P_{lat} A-P translation, with overall mean SDs of only 0.8–2.0 mm across all repetitions of each different task (Figs. S2–S4).

For comparison, the N_Ps were located anteriorly (N_P_{med}: 4.7 ± 5.4 mm; N_P_{lat}: 11.3 ± 9.7 mm) to the mid-coronal plane while standing. As opposed to the FFA_P, a considerable difference between the A-P translations of N_P_{med} compared to N_P_{lat} was found for both phases of all three activities (Table 1C). While N_P_{med} showed a consistent pattern of A-P translation for all subjects over all activities, high inter-subject variability was observed for N_P_{lat}, especially during mid-stance of level walking and shortly before heel-strike in all activities (Fig. 4). However, the mean intra-subject variability (1.2–3.0 mm) was comparable to both FFA points throughout the entire gait cycles (Figs. S2–S4).

3.3. CoR in the transverse plane

Over all subjects, a slightly medial mean CoR was observed for the entire gait cycle of all activities with the swing phase (level walking: 13.7 ± 14.4 mm; downhill walking: 11.7 ± 9.0 mm; stair descent: 14. 6 ± 9.8 mm, all medial) nearly always presenting a more medial CoR than the stance phase (level walking: 7.2 ± 7.4 mm; downhill walking: 6.7 ± 8.8 mm; stair descent: 9.4 ± 14.3 mm, all medial) (Fig. 5, Tables S1–S3). Intra-subject variability of the location of the FFA_P_{med} and FFA_P_{lat} within a task was high (Figs. S5–S34), and resulted in SD's ranging from 0.9 to 23.3 mm for the mean location of the subject-specific CoR over a gait phase (Tables S1–S3).

4. Discussion

A comprehensive understanding of human knee joint kinematics is critical for guiding the design of total knee replacement components that aim to mimic healthy joint motion. Until now, movement of the tibio-femoral joint has been discussed controversially, but only rarely analysed over multiple cycles of different activities. For the first time in healthy knees, moving fluoroscopy has been used in this study to determine the *in vivo* tibio-femoral rotations and translations that occur throughout complete cycles of downhill walking and stair descent, in addition to free level walking, using the same subject cohort as well as the same measurement set-up. Only a limited task-dependency was observed for ranges of A-P translation, despite clear differences in knee flexion angles (Table 1). Overall, the data have revealed a predominantly central to medial CoR in the transverse plane, even though it is located laterally in some individuals and during some phases of different activity cycles.

The flexion/extension patterns during level walking found in this study were consistent with those reported in the literature (Gray et al., 2019; Lafortune et al., 1992). Furthermore, our tibio-femoral internal-external rotation patterns were comparable to the limited evidence available on complete gait cycles during level walking (Gray et al., 2019), even though the absolute values differed. This variation likely originates from differences in the definition of the femoral and tibial anatomical coordinate systems (Gray et al., 2019; Lafortune et al., 1992). In our study, similar ranges of A-P translation were observed for both compartments (using FFA_P_{med} and FFA_P_{lat}), but with larger A-P translations on the lateral side of the joint for the unloaded swing phase of level walking and stair descent. Such data is consistent with previous studies that suggested a medial pivot during unloaded flexion (Iwaki et al., 2000; Pinskerova et al., 2004). The magnitude of the overall translations of the medial compartment (FFA_P_{med}) were comparable to values presented in the literature, whereas for the lateral compartment (FFA_P_{lat}), contradictory results were found (Gray et al., 2019; Kozanek et al., 2009). As the subject-specific FFA was optimised over the full range of motion during deep knee bending,

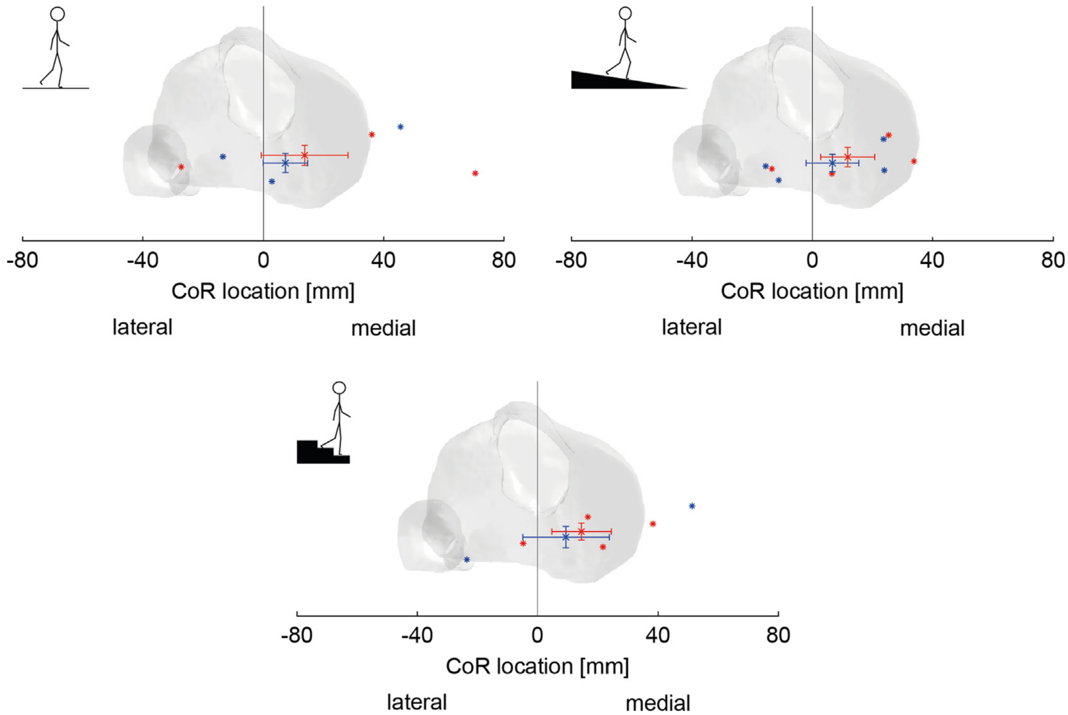

Fig. 5. Location of the centre of rotation (CoR) shown on the plateau of a left tibia during the loaded stance (blue) and the unloaded swing (red) phases of level walking (top left), downhill walking (top right) and stair descent (bottom). The mean across all subjects as well as the standard deviations in the antero-posterior and medio-lateral directions are indicated with whiskers. The most extreme points in each direction across all subjects and trials are presented as *.

the true instantaneous flexion axis at a specific instant of time might vary from the mean FFA, possibly introducing an A-P translation error around the flexion axis. Further investigation is clearly required in order to understand the influence of such secondary errors, including their role relative to different activities and flexion axis approaches.

To allow cross-study comparison, we have also presented condylar kinematics using the nearest point approach. While the range of A-P translation for some subjects was in line with the literature (Gray et al., 2019), others exhibited a substantially larger range of A-P translation. An assessment of the femoral geometries revealed a relatively flat region on the lateral condyle (similar to previous observations in cadaveric studies (Iwaki et al., 2000)) for some subjects, plausibly resulting in a "jump" of the N_P_{lat} during phases of knee extension (Fig. 4, right). As a result, it seems that this method is sensitive to local contact conditions, but does not necessarily describe the relative movement between the tibia and the femur. Additional research into the influence of subject-specific anatomy on the translation of the contact points is thus needed before a thorough understanding of the large variability in A-P translation between subjects can be gained.

The mean CoR was located on the medial tibial plateau for all three activities. Nevertheless, the location of trial specific mean CoRs varied among subjects and tasks (Tables S1–S3). These results are generally in line with previous findings (Dennis et al., 2001; Gray et al., 2019), although a mean lateral CoR has also been presented (Koo and Andriacchi, 2008; Kozanek et al., 2009). Calculation of the mean CoR over the complete gait cycle seems to be more robust than for either the stance or swing phase individually, resulting in SDs of less than 5 mm for most of the subjects, in line with previous research (Dennis et al., 2001). Furthermore, individual movement patterns were clearly observed, thus emphasising the need to analyse multiple trials for individual subjects.

Overall, the majority of studies fail to capture the unloaded stance phase, which, based on the results of our study, differs from the loaded stance phase. Analysis of this phase of gait provides clear insights into the largest joint rotations that are critical for understanding soft tissue loading as well as possible overloading (Hosseini Nasab et al., 2019, 2020). Accurate assessment of complete cycles of daily activities could therefore be key for planning subject-specific component implantation to achieve pain-free post-operative outcome.

Walking with the moving fluoroscope potentially influenced the natural gait patterns of our subjects in the present study, especially as walking speeds are known to be reduced compared to free level walking (Stacoff et al., 2005). However, the changes in gait parameters have been shown to be small, and gait patterns remain comparable to those exhibited during slow walking (Hitz et al., 2018). While kinematics captured in this study may not be completely natural, they still represent the state-of-the-art in understanding joint motion over complete cycles and for different daily activities. The predominant drawback, however, is the subject's exposure to radiation, necessitating that data collection using such technologies is kept to a minimum.

Overall, comparison with the existing literature is challenging, mainly due to the variety of approaches used. While the geometric centre axis as well as the transepicondylar axis are widely used, their definition is highly dependent on the protocol and experience of the examiner. Within this study, we aimed to minimise the observers input to receive an independent axis that is only based on the subject's deep knee bending movement (using the fluoroscopic based reconstruction of the bone segments). Only the tibial coordinate system in our study was defined based on subject-specific anatomy, but it is indeed entirely plausible that individual differences could have added variation to the presented results.

Although the current single-plane set-up in combination with the semi-automatic 2D/3D registration possesses high accuracy in the in-plane direction (Postolka et al., 2020), a combination of errors for different segments could plausibly lead to larger total relative errors. The greatest source of error is likely to arise from the contralateral knee crossing through the image twice during each gait cycle, hence cumulatively limiting the accuracy of the 2D/3D registration at these instances. In addition, out-of-plane registration errors could play a role in the determination of the CoR in the transverse plane. To overcome this limitation as well as to improve out-of-plane accuracy, a dual-plane set-up could provide considerable advantages, however this would increase the overall radiation dosage applied to the subject.

This study provides the first analysis of knee kinematics during multiple complete cycles of free level walking, downhill walking and stair descent. The results suggest that the CoR is primarily located medially, but varies between subjects and gait phases. It therefore seems that the recent movement towards medial congruent implant designs (Schütz et al., 2019) is warranted, but further investigation is clearly needed to elucidate the role of limb alignment and anatomical inter-subject variability on knee joint kinematics, particularly with regard to the loading and possible overloading of the surrounding soft tissues (Hosseini Nasab et al., 2019). Importantly, however, the subject-specific movement patterns observed in this study indicate that individual implant selection and/or surgical implantation decisions might be necessary before further improvement to joint replacement outcome can be achieved, possibly supported by the accurate assessment of each individual's pre-operative knee joint kinematics to guide clinical decision-making.

Acknowledgement

The study was partially financed by the Commission for Technology and Innovation (Bern, Switzerland, Project Number 17078.1 PFLS-LS) and Medacta International SA (Castel San Pietro, Switzerland). The sponsor was not involved in the data collection, nor in the analysis or the interpretation of the data. Furthermore, the authors would like to thank all the subjects who participated in the study, as well as Nathalie Kühne (Balgrist University Hospital, Zürich, Switzerland) for the organisation of the clinical examinations and all the students for their help in the data collection.

Conflict of interest statement

The authors declare the following financial interests/personal relationships which may be considered as potential competing interests: RL has received speaker's fees from Medacta. SFF and VP receive advisory fees from Medacta as part of their consultancy work. MARF has received consultancies from Medacta.

Appendix A. Supplementary material

Supplementary data to this article can be found online at https://doi.org/10.1016/j.jbiomech.2020.109915.

References

Akbarshahi, M., Schache, A.G., Fernandez, J.W., Baker, R., Banks, S., Pandy, M.G., 2010. Non-invasive assessment of soft-tissue artifact and its effect on knee joint kinematics during functional activity. J. Biomech. 43, 1292–1301.

Anderst, W., Zauel, R., Bishop, J., Demps, E., Tashman, S., 2009. Validation of three-dimensional model-based tibio-femoral tracking during running. Med. Eng. Phys. 31, 10–16.

Andriacchi, T.P., Alexander, E.J., Toney, M.K., Dyrby, C., Sum, J., 1998. A point cluster method for in vivo motion analysis: applied to a study of knee kinematics. J. Biomech. Eng. 120, 743–749.

Asano, T., Akagi, M., Tanaka, K., Tamura, J., Nakamura, T., 2001. In vivo three-dimensional knee kinematics using a biplanar image-matching technique. Clin. Orthop. Relat. Res., 157–166

Banks, S.A., Hodge, W.A., 1996. Accurate measurement of three-dimensional knee replacement kinematics using single-plane fluoroscopy. IEEE Trans. Biomed. Eng. 43, 638–649.

Benoit, D.L., Ramsey, D.K., Lamontagne, M., Xu, L., Wretenberg, P., Renstrom, P., 2007. In vivo knee kinematics during gait reveals new rotation profiles and smaller translations. Clin. Orthop. Relat. Res. 454, 81–88.

Cappozzo, A., Croce, U.D., Leardini, A., Chiari, L., 2005. Human movement analysis using stereophotogrammetry. Part 1: theoretical background. Gait Posture 21, 186–196.

Dennis, D., Komistek, R., Scuderi, G., Argenson, J.N., Insall, J., Mahfouz, M., Aubaniac, J.M., Haas, B., 2001. In vivo three-dimensional determination of kinematics for subjects with a normal knee or a unicompartmental or total knee replacement. J Bone Joint Surg Am 83-A (Suppl 2 Pt 2), 104–115.

Ehrig, R.M., Taylor, W.R., Duda, G.N., Heller, M.O., 2006. A survey of formal methods for determining the centre of rotation of ball joints. J. Biomech. 39, 2798–2809.

Ehrig, R.M., Taylor, W.R., Duda, G.N., Heller, M.O., 2007. A survey of formal methods for determining functional joint axes. J. Biomech. 40, 2150–2157.

Farrokhi, S., Tashman, S., Gil, A.B., Klatt, B.A., Fitzgerald, G.K., 2012. Are the kinematics of the knee joint altered during the loading response phase of gait in individuals with concurrent knee osteoarthritis and complaints of joint instability? A dynamic stereo X-ray study. Clin. Biomech. (Bristol, Avon) 27, 384–389.

Farrokhi, S., Voycheck, C.A., Klatt, B.A., Gustafson, J.A., Tashman, S., Fitzgerald, G.K., 2014. Altered tibiofemoral joint contact mechanics and kinematics in patients with knee osteoarthritis and episodic complaints of joint instability. Clin. Biomech. (Bristol, Avon) 29, 629–635.

Folinais, D., Thelen, P., Delin, C., Radier, C., Catonne, Y., Lazennec, J.Y., 2013. Measuring femoral and rotational alignment: EOS system versus computed tomography. Orthop. Traumatol. Surg. Res. 99, 509–516.

Foresti, M., 2009. In Vivo Measurement of Total Knee Joint Replacement Kinematics and Kinetics During Stair Descent. PhD Thesis, ETH Zurich, Zurich.

Galvin, C.R., Perriman, D.M., Lynch, J.T., Pickering, M.R., Newman, P., Smith, P.N., Scarvell, J.M., 2019. Age has a minimal effect on knee kinematics: a cross-sectional 3D/2D image-registration study of kneeling. Knee 26, 988–1002.

Gray, H.A., Guan, S., Thomeer, L.T., Schache, A.G., de Steiger, R., Pandy, M.G., 2019. Three-dimensional motion of the knee-joint complex during normal walking revealed by mobile biplane X-ray imaging. J. Orthop. Res. 37 (3), 615–630. https://doi.org/10.1002/jor.24226.

Grieco, T.F., Sharma, A., Dessinger, G.M., Cates, H.E., Komistek, R.D., 2018. In vivo kinematic comparison of a bicruciate stabilized total knee arthroplasty and the normal knee using fluoroscopy. J. Arthroplasty 33, 565–571.

Grieco, T.F., Sharma, A., Komistek, R.D., Cates, H.E., 2016. Single versus multiple-radii cruciate-retaining total knee arthroplasty: an in vivo mobile fluoroscopy study. J. Arthroplasty 31, 694–701.

Grood, E.S., Suntay, W.J., 1983. A joint coordinate system for the clinical description of three-dimensional motions: application to the knee. J. Biomech. Eng. 105, 136–144.

Guan, S., Gray, H.A., Keynejad, F., Pandy, M.G., 2016. Mobile biplane X-ray imaging system for measuring 3D dynamic joint motion during overground gait. IEEE Trans. Med. Imaging 35, 326–336.

Guan, S., Gray, H.A., Schache, A.G., Feller, J., de Steiger, R., Pandy, M.G., 2017. In vivo six-degree-of-freedom knee-joint kinematics in overground and treadmill walking following total knee arthroplasty. J. Orthop. Res. 35, 1634–1643.

Hitz, M., Schütz, P., Angst, M., Taylor, W.R., List, R., 2018. Influence of the moving fluoroscope on gait patterns. PLoS ONE 13, e0200608. https://doi.org/10.1371/journal.pone.0200608. https://journals.plos.org/plosone/article?id=10.1371/journal.pone.0200608. 30005086.

Hosseini Nasab, S.H., Smith, C.R., Schütz, P., Damm, P., Trepczynski, A., List, R., Taylor, W.R., 2020. Length-change patterns of the collateral ligaments during functional activities after total knee arthroplasty. Ann Biomed Eng 48 (4), 1396–1406. https://doi.org/10.1007/s10439-020-02459-3.

Hosseini Nasab, S.H., Smith, C.R., Schütz, P., Postolka, B., List, R., Taylor, W.R., 2019. Elongation patterns of the collateral ligaments after total knee arthroplasty are dominated by the Knee Flexion Angle. Front Bioeng. Biotechnol. 7. https://doi.org/10.3389/fbioe.2019.00323. https://www.frontiersin.org/articles/10.3389/fbioe.2019.00323/full. 31799245.

Iwaki, H., Pinskerova, V., Freeman, M.A.R., 2000. Tibiofemoral movement 1: the shapes and relative movements of the femur and tibia in the unloaded cadaver knee. J. Bone Joint Surg.-British 82B, 1189–1195.

Komistek, R.D., Dennis, D.A., Mahfouz, M., 2003. In vivo fluoroscopic analysis of the normal human knee. Clin. Orthop. Relat. Res., 69–81

Kono, K., Tomita, T., Futai, K., Yamazaki, T., Tanaka, S., Yoshikawa, H., Sugamoto, K., 2018. In vivo three-dimensional kinematics of normal knees during different high-flexion activities. Bone Joint J. 100b, 50–55.

Koo, S., Andriacchi, T.P., 2008. The knee joint center of rotation is predominantly on the lateral side during normal walking. J. Biomech. 41, 1269–1273.

Kozanek, M., Hosseini, A., Liu, F., Van de Velde, S.K., Gill, T.J., Rubash, H.E., Li, G., 2009. Tibiofemoral kinematics and condylar motion during the stance phase of gait. J. Biomech. 42, 1877–1884.

Lafortune, M.A., Cavanagh, P.R., Sommer 3rd, H.J., Kalenak, A., 1992. Three-dimensional kinematics of the human knee during walking. J. Biomech. 25, 347–357.

Li, G., Kozanek, M., Hosseini, A., Liu, F., Van de Velde, S.K., Rubash, H.E., 2009. New fluoroscopic imaging technique for investigation of 6DOF knee kinematics during treadmill gait. J. Orthop. Surg. Res. 4, 6.

Li, G., Van de Velde, S.K., Bingham, J.T., 2008. Validation of a non-invasive fluoroscopic imaging technique for the measurement of dynamic knee joint motion. J. Biomech. 41, 1616–1622.

List, R., Gulay, T., Stoop, M., Lorenzetti, S., 2013. Kinematics of the trunk and the lower extremities during restricted and unrestricted squats. Journal of Strength and Conditioning Research 27 (6), 1529–1538. https://doi.org/10.1519/Jsc.0b013e3182736034.

List, R., Postolka, B., Schütz, P., Hitz, M., Schwilch, P., Gerber, H., Ferguson, S.J., Taylor, W.R., 2017. A moving fluoroscope to capture tibiofemoral kinematics during complete cycles of free level and downhill walking as well as stair descent. PLoS One 12 (10). https://doi.org/10.1371/journal.pone.0185952.

Moewis, P., Duda, G.N., Jung, T., Heller, M.O., Boeth, H., Kaptein, B., Taylor, W.R., 2016. The restoration of passive rotational tibio-femoral laxity after anterior cruciate ligament reconstruction. PLoS ONE 11, e0159600.

Moro-oka, T.A., Hamai, S., Miura, H., Shimoto, T., Higaki, H., Fregly, B.J., Iwamoto, Y., Banks, S.A., 2008. Dynamic activity dependence of in vivo normal knee kinematics. J. Orthop. Res. 26, 428–434.

Pauchard, Y., Fitze, T., Browarnik, D., Eskandari, A., Pauchard, I., Enns-Bray, W., Palsson, H., Sigurdsson, S., Ferguson, S.J., Harris, T.B., Gudnason, V., Helgason, B., 2016. Interactive graph-cut segmentation for fast creation of finite element models from clinical ct data for hip fracture prediction. Comput. Methods Biomech. Biomed. Eng. 19, 1693–1703.

Pinskerova, V., Johal, P., Nakagawa, S., Sosna, A., Williams, A., Gedroyc, W., Freeman, M.A., 2004. Does the femur roll-back with flexion?. J. Bone Joint Surg. Br. 86, 925–931.

Postolka, B., List, R., Thelen, B., Schütz, P., Taylor, W.R., Zheng, G., 2020. Evaluation of an intensity-based Algorithm for 2D/3D Registration of Natural Knee Videofluoroscopy Data. Med. Eng. Phys. 77, 107–113, 31980316. https://doi.org/10.1016/j.medengphy.2020.01.002.

Reinschmidt, C., vandenBogert, A.J., Lundberg, A., Nigg, B.M., Murphy, N., Stacoff, A., Stano, A., 1997. Tibiofemoral and tibiocalcaneal motion during walking: external vs. skeletal markers. Gait Posture 6, 98–109.

Schütz, P., Postolka, B., Gerber, H., Ferguson, S.J., Taylor, W.R., List, R., 2019. Knee implant kinematics are task-dependent. J. R. Soc. Interface 16 (151), 20180678. https://doi.org/10.1098/rsif.2018.0678.

Schütz, P., Taylor, W.R., Postolka, B., Fucentese, S.F., Koch, P.P., Freeman, M.A.R., Pinskerova, V., List, R., 2019. Kinematic evaluation of the GMK sphere implant during gait activities: a dynamic videofluoroscopy study. J. Orthop. Res. 37 (11), 2337–2347. https://doi.org/10.1002/jor.24416.

Stacoff, A., Diezi, C., Luder, G., Stussi, E., Kramers-de Quervain, I.A., 2005. Ground reaction forces on stairs: effects of stair inclination and age. Gait Posture 21, 24–38.

Taylor, W.R., Ehrig, R.M., Duda, G.N., Schell, H., Seebeck, P., Heller, M.O., 2005. On the influence of soft tissue coverage in the determination of bone kinematics using skin markers. J. Orthop. Res. 23, 726–734.

Yamaguchi, S., Gamada, K., Sasho, T., Kato, H., Sonoda, M., Banks, S.A., 2009. In vivo kinematics of anterior cruciate ligament deficient knees during pivot and squat activities. Clin. Biomech. (Bristol, Avon) 24, 71–76.

Yamokoski, J.D., Banks, S.A., 2011. Does close proximity robot motion tracking alter gait?. Gait Posture 34, 508–513.